RSC Advances

ROYAL SOCIETY OF CHEMISTRY

www.rsc.org/advances

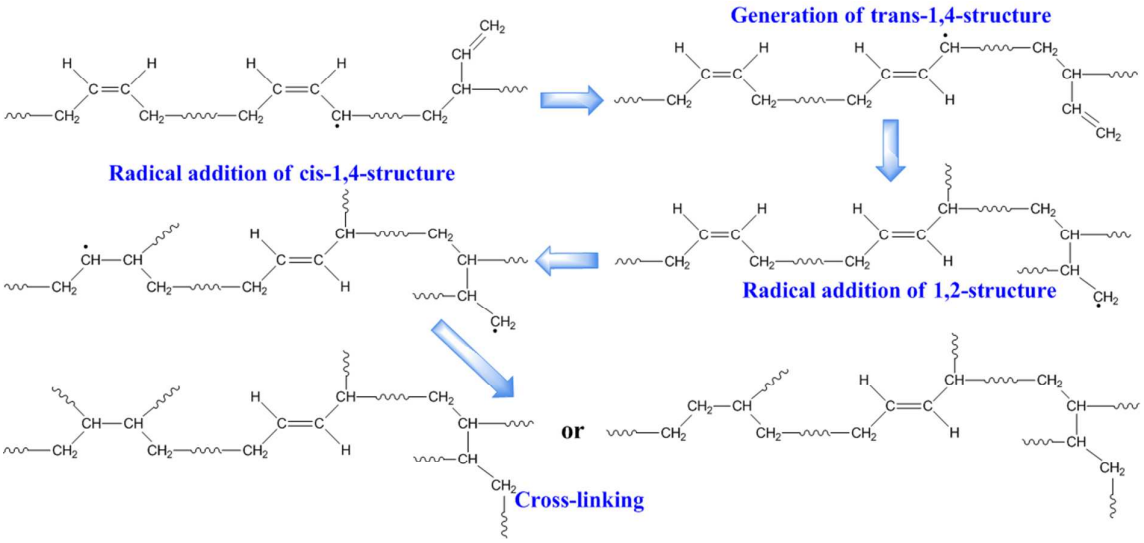

Detailed mechanism of cis-BR cross-linking with peroxides was studied using PCMD2D and 2D correlation FTIR, and 5-steps process was determined.

RSC Advances

RSC Publishing

ARTICLE

Cross-linking Process of Cis-Polybutadiene Rubber with Peroxides Studied by Two-dimensional Infrared Correlation Spectroscopy: a Detailed Tracking

Xifei Liu,[a] Tao Zhou,[a,*] Yongcheng Liu,[a] Aiming Zhang,[a,*] Canyao Yuan,[b] and Weidong Zhang[b]

Cite this: DOI: 10.1039/xoxxoooooox

Received ooth January 2012,
Accepted ooth January 2012

DOI: 10.1039/xoxxoooooox

www.rsc.org/

Cis-polybutadiene rubber (cis-BR) is one of the typical unsaturated rubbers in a mass production and widely used. However, the detailed mechanism of its cross-linking with peroxides has been still unclear so far. In this study, in situ FTIR spectra combined with the powerful PCMD2D and 2D correlation spectroscopy was used to track the detailed cross-linking process. The temperature region of cis-BR cross-linking determined by PCMW2D was within 165-195 °C. The temperature with a maximum cross-linking rate was determined at 183 °C via PCMW2D, which is identical with DSC. The generation of –ĊH– macromolecular free radicals through losing α hydrogens was observed when below 165 °C. An abnormal increasing of double bonds with trans-1,4-structure during the cross-linking (165-195 °C) was observed. It also found an obvious enhancement of $-CH_2-$ groups, which indicated that a large part of the double bonds with cis-1, 4- and 1, 2-structrue involved in cross-linking is transformed to $-CH_2-$ groups. A 5-steps process for the whole cross-linking was inferred from the sequential orders of group motions. The first step is DCP decomposition and the free radicals releasing. The second step is the generation of trans-1,4-structure due to the internal rotation of cis-1,4-structure induced by free radicals at α position. The third step is the free radical addition of double bonds with 1,2-structure, and the fourth is the free radical addition of double bonds with cis-1,4-structure. The final step is the cross-linking via double coupling of two macromolecular free radicals. In the last step, the free radicals from cis-1,4-structure also can be probably terminated by a chain transfer.

1. Introduction

Rubber materials are one of the most important feedstocks in modern industry. Since the molecular structure of Natural Rubber (NR) was determined by Michael Farady in 1826 and Greville Williams in 1860,[1] a series of rubbers have been synthesized so far, such as polybutadiene rubber (BR), styrene-butadiene rubber (SBR), chloroprene rubber (CR), nitrile butadiene rubber (NBR), polysulfide rubber, and butyl rubber.[1] After the invention of anionic polymerization and coordination polymerization, stereoregularity rubbers also begin to produce in industry, such as polyisoprene rubber (PI),[2] polybutadiene rubber, ethylene-propylene rubber (EPR), and solution polymerization styrene-butadiene rubber (S-SBR).

The cross-linking is most important for the conventional rubber materials. Linear structure of rubber molecular chain is transformed into a three-dimensional network structure during a cross-linking process, resulting in the rubber entropy elasticity and a high mechanical strength.[3, 4] Scientists have been found that different cross-linking systems give different properties to rubbers. For traditional sulfur cross-linking system, excellent mechanical properties, a high flexibility and a high elongation at break, can be obtained because of the generation of multi-sulfur bonds $-S_x-$.[5, 6] For peroxides cross-linking system, superior combination properties, including a high mechanical strength, a good wear resistance, a high thermal oxidation stability, and a low compression set, are gained due to the formation of C–C bonds.[7] Although peroxide cross-linkers are usually used in saturated rubbers (e.g., EPR), nowadays, because of a higher requirement of mechanical properties for unsaturated rubbers, peroxide cross-linkers have also been more and more used in unsaturated rubber materials instead of the sulfur.[8-11] Cis-polybutadiene rubber (cis-BR) is one of the typical unsaturated rubbers in a mass production and widely used in large-scale components just like tires and conveyors. Classical theory suggests that the peroxide first decomposes into radicals under heating, and then macromolecular radicals

of cis-BR are generated by these radicals through capturing the α hydrogen of cis-BR backbone or the addition reaction of a double bond.[12-14] However, cis-BR contains two types of double bonds and a type of α hydrogens due to cis-1, 4- and 1, 2-structure (see **Scheme 1**).[15, 16] The way of the formation of cross-linked C–C bonds from these reactive functional groups has been still unclear in the cross-linking process. A depth understanding of the mechanism of cis-BR cross-linking has an important scientific and practical value. It is also significant to understand the cross-linking process of BR with a high 1, 2-structure content which is currently used more and more in tires because of the low heat generation.

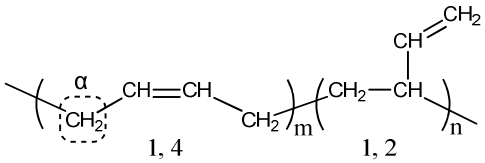

Scheme 1. Molecular structure of cis-polybutadiene.

Generalized two-dimensional (2D) correlation infrared spectroscopy which is a widely used spectroscopy method was proposed by Noda in 1993.[17] In this method, the sequential order of spectral variables can be easily obtained according to Noda's rules. So the mechanism of polymer transitions and molecular interactions can be conveniently studied by using 2D correlation infrared spectroscopy. In order to determine the transition temperature of a thermotropic liquid-crystal sample, Thomas and Richardson[18] proposed moving-window two-dimensional correlation spectroscopy (MW2D) in 2000. In 2006, Morita proposed a new method based on the MW2D, which is called perturbation-correlation moving-window two-dimensional correlation spectroscopy (PCMW2D).[19] Spectral correlation variations along both perturbation variables (e.g., temperature) and spectral variables (e.g., wavenumber) axis can be direct observed in the PCMW2D spectra.[19-23] In the past five years, researchers found that the combination of PCMW2D and generalized 2D correlation spectroscopy was the best way.[21-23] In general, PCMW2D was employed to determine the transition point and the transition range of polymers; then, generalized 2D spectroscopy was performed to study the mechanism of functional groups at a specific transition.[24-29] Many successful applications were reported in the study of the mechanism of polymer physical or chemical transitions.[30-36]

In this study, the cross-linking process of cis-BR induced by peroxide is investigated by in situ FTIR spectroscopy combined with 2D correlation analysis. The differential scanning calorimeter (DSC) is also used to assist the determination of the temperature region of the cross-linking process. A series of reactions on α hydrogens, and double bonds of 1, 4- and 1, 2-structrue is successfully observed. Meanwhile, the generation of new $-CH_2-$ groups can be determined. Also, the sequential orders of these functional groups involved during the cross-linking reaction are elucidated, indicating a depth understanding of the mechanism.

2. Experimental

2.1. Materials

The cis-polybutadiene rubber (cis-BR) used in this experiment was kindly supplied by Jilin Petrochemical Company. Dicumyl peroxide (DCP) was purchased from Kelong Reagent and Chemical Plant with an AR grade. The number-average molecular weight of cis-BR was 120000 g/mol using GPC measurement (tetrahydrofuran as a mobile phase) and M_w/M_n=3.41. The content of cis-1, 4, trans-1, 4, and 1, 2-structure were 94.5%, 2.3%, and 3.2% (see Supporting Information for calculation method), which were measured using ^{1}H NMR and inverse gated decoupling ^{13}C NMR. The ^{1}H NMR spectrum and ^{13}C NMR spectrum are provided in **Figure S1** and **Figure S2** in the Supporting Information. The assignments of the shift in NMR spectra are also provided in **Table S1** in the Supporting Information. The melting point of pure cis-BR used here was 2 °C (DSC).

2.2. Sample preparation

The cis-BR and DCP were mixed by using a laboratory two-roll mill at a room temperature without any other chemical reagents. To ensure a clear display of DCP in the FTIR spectrum, the weight ratios of cis-BR and DCP were 100 and 5, respectively.

2.3. DSC measurement

DSC was performed on NETZSCH DSC 204 F1. The sample was direct heated from 30 °C to 240 °C at 10 °C/min. The sample was protected by a high-purity nitrogen atmosphere (50 ml/min).

2.4. FTIR spectroscopy upon heating

BR/DCP blend was first dissolved in the cyclohexane. The FTIR sample was spread on one side of a KBr disk (0.8 mm thick) by solvent casting from 200 g/L cyclohexane solution. The sample was first placed at room temperature in air for 15 min to naturally evaporate most of the solvent, and then was dried in a vacuum around 40 °C to evaporate the residual solvent. After that, the sandwiched sample was obtained by covering with another KBr disk to prevent from flowing during the heating process. The sandwiched sample was placed into a homemade temperature control equipment including a program heating and cooling unit. The temperature-dependent absorbance FTIR spectra were collected with Nicolet iS10 FTIR spectrometer, equipped with a deuterated triglycine sulfate (DTGS) detector. The sample was heated from 50 °C to 220 °C at 5 °C/min, and a total of 99 FTIR spectra were collected. The spectral resolution was 4 cm^{-1}, and the scans of each spectrum were 20. The sample was protected by a dried high-purity nitrogen gas with 300 ml/min during the measurement.

2.5. 2D correlation analysis

PCMW2D and generalized 2D correlation FTIR spectra were processed and calculated by 2DCS, developed by one of the authors. The linear baseline corrections were applied in the region of 3140−2590 cm^{-1}, 1540−890 cm^{-1}, and 890−530 cm^{-1} before 2D correlation analysis. The window size was chosen as 11 (*2m+1*) to produce high-quality PCMW2D spectra. The 3% autocorrelation intensity of spectra was regarded as noise and was cut off. In 2D correlation FTIR spectra, the pink areas represent positive correlation intensity, and the blue areas represent the negative correlation intensity. The detailed theory and algorithm of PCMW2D and generalized 2D correlation spectroscopy can refer to the literature.[19, 33, 37] Here, the basic theory of PCMW2D is introduced as follows.

A(v,I) is a *M*×*N* spectral intensity matrix, where *v* and *I* are the spectral variable (wavenumber) and the perturbation variable (temperature), respectively. $a_j(v,I)$ is a submatrix which is extracted from the *j*th row of *A(v,I)*. $a_j(v,I)$ has *2m+1* rows. Here, *2m+1* is called as the window size.

$$a_j(v,I)=\begin{pmatrix} y(v_1,I_{j-m}) & y(v_2,I_{j-m}) & \cdots & y(v_N,I_{j-m}) \\ \vdots & \vdots & \cdots & \vdots \\ y(v_1,I_j) & y(v_2,I_j) & \cdots & y(v_N,I_j) \\ \vdots & \vdots & \cdots & \vdots \\ y(v_1,I_{j+m}) & y(v_2,I_{j+m}) & \cdots & y(v_N,I_{j+m}) \end{pmatrix} \quad (1)$$

The reference spectrum and dynamic spectum of $a_j(v,I)$ can be calculated as follows.

$$\bar{y}(v)=\frac{1}{2m+1}\sum_{J=j-m}^{j+m} y(v,I_J) \quad (2)$$

$$\tilde{y}(v,I_J)=y(v,I_J)-\bar{y}(v) \quad (3)$$

The dynamic perturbation is calculated below.

$$\bar{I}_j=\frac{1}{2m+1}\sum_{J=j-m}^{j+m} I_J \quad (4)$$

$$\tilde{I}_J=I_J-\bar{I}_j \quad (5)$$

The mean-centered *j*th submatrix is obtained.

$$\tilde{a}_j(v,I)=\begin{pmatrix} \tilde{y}(v_1,I_{j-m}) & \tilde{y}(v_2,I_{j-m}) & \cdots & \tilde{y}(v_N,I_{j-m}) \\ \vdots & \vdots & \cdots & \vdots \\ \tilde{y}(v_1,I_j) & \tilde{y}(v_2,I_j) & \cdots & \tilde{y}(v_N,I_j) \\ \vdots & \vdots & \cdots & \vdots \\ \tilde{y}(v_1,I_{j+m}) & \tilde{y}(v_2,I_{j+m}) & \cdots & \tilde{y}(v_N,I_{j+m}) \end{pmatrix} \quad (6)$$

Synchronous and asynchronous PCMW2D spectra of mean-centered *j*th submatrix are calculated according to Eqs. (7) and (8).

$$\Pi_{\Phi,j}(v,I_j)=\frac{1}{2m}[\tilde{a}_j(v,I)]^T\cdot\tilde{I}_J \quad (7)$$

$$\Pi_{\Psi,j}(v,I_j)=\frac{1}{2m}[\tilde{a}_j(v,I)]^T\cdot H\cdot\tilde{I}_J \quad (8)$$

where the superscript *T* represents the matrix transpose. *H* is the Hilbert-Noda transformation matrix[17, 19] which is defined as:

$$h_{ik}=\begin{cases} 0 & i=k \\ \frac{1}{\pi(k-i)} & otherwise \end{cases} \quad (9)$$

where h_{ik} is the element of the *i*th row and the *k*th column of *H*. The synchronous and asynchronous PCMW2D spectra are gained through sliding submatrix position from *j=1+m* to *M−m* and repeating calculations of Eqs. (1)-(9) at each submatrix.

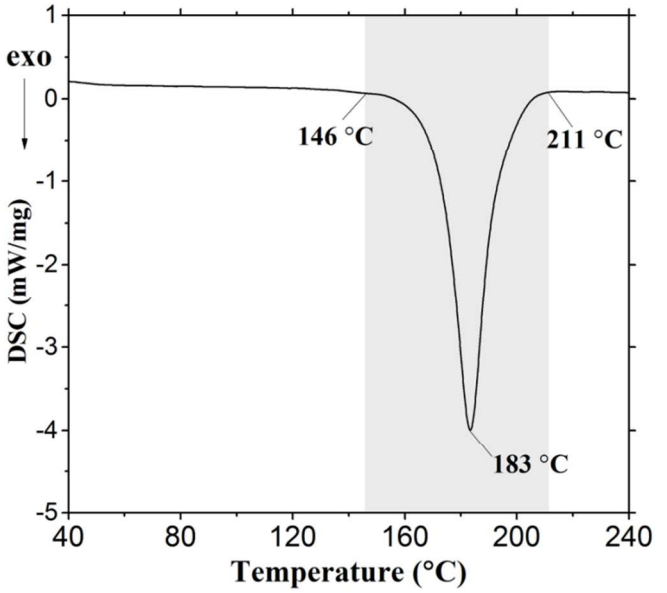

Figure 1. DSC curve of the cross-linking process of cis-BR with dicumyl peroxide.

Table.1 Assignments and the explanation of FTIR bands of cis-BR and DCP.

wavenumber (cm^{-1})	assignments
3006	*v*(=C−H, 1,4), C−H stretching of 1,4-structure (*cis*+*trans*)
2932	v_{as}(−CH_2−), C−H asymmetrical stretching of −CH_2−groups
2852	v_s(−CH_2−), C−H symmetrical stretching of −CH_2−groups
1152	*v*(−C−O−, DCP), −C−O− stretching of peroxy in DCP
993	γ(=C−H, 1,2-), C−H rocking of 1,2-structure
965	γ(=C−H, *trans*-1,4), C−H rocking of *trans*-1,4-structure
910	γ(=C−H, 1,2-), C−H rocking of 1,2-structure
762	δ(=C−H, DCP), C−H bending of benzene rings in DCP
697	δ(=C−H, DCP), C−H bending of benzene rings in DCP
738	γ(=C−H, *cis*-1,4), C−H rocking of *cis*-1,4-structure

3. Results and Discussion

3.1. Cross-linking process measured by DSC

Cross-linking reaction is generally exothermic, and therefore, the temperature range of the cross-linking process can be determined by DSC measurement. **Figure 1** illustrates DSC curve of the crosslinking of cis-BR induced by dicumyl peroxide upon heating (10 °C/min). An exothermic peak at 183 °C is observed, and the temperature range of this peak is from 146 °C to 211 °C. It indicates that the cross-linking reaction begins at 146 °C and ends at 211 °C, and 183 °C is the temperature with the maximum reaction rate. However, no other peaks are observed when the temperature is below 146 °C.

3.2. In situ FTIR spectroscopy

The temperature-dependent FTIR spectra of the cross-linking process of cis-BR from 50 °C to 220 °C are shown in **Figure 2** (also see **Figure S3** in the Supporting Information). Only a part of spectra are displayed for clarity. The assignments of the interesting bands in the present study are listed in **Table 1**.[38-41] As shown in **Figure 2(a)**, the intensities of the peaks at 2932 cm^{-1} and 2852 cm^{-1} gradually increases with the temperature increasing from 50 °C to 220 °C. At the same time, the intensity of the peak at 3006 cm^{-1} decreases. The peaks at 2932 cm^{-1} and 2852 cm^{-1} are assigned to C−H asymmetrical stretching and symmetrical stretching of $-CH_2-$ groups, respectively. This indicates the enhancement of the molar concentration of $-CH_2-$ groups during the cross-linking process. The peak at 3006 cm^{-1} is attributed to =C−H stretching of 1,4-structure. The decreasing of 3006 cm^{-1} indicates the reaction of the double bonds in the cross-linking process, showing a disappearance of a part of the double bonds with 1,4-structure.

In the experimental section, the results of NMR determined that the content of cis-1, 4, trans-1, 4, and 1, 2-structure of cis-BR were 94.5%, 2.3%, and 3.2%, respectively. As shown in **Figure 2(c)**, the temperature-dependent FTIR spectra in the region 1000–650 cm^{-1} also clearly detect these structures. The peaks at 993 cm^{-1} and 910 cm^{-1} are assigned to =C−H rocking of 1,2-structure, and the peak at 965 cm^{-1} is attributed to =C−H rocking of trans-1,4-structure. The peak at 738 cm^{-1} is the =C−H rocking of cis-1,4-structure. It can be clearly observed that the intensities of 993 cm^{-1}, 910 cm^{-1}, and 738 cm^{-1} gradually decrease with the temperature increasing, indicating the reactions of double bonds of cis-1,4-structure and 1,2-structure during the cross-linking. However, the intensity of 965 cm^{-1} abnormally enhances at the same time. This shows the concentration of double bonds of trans-1,4-structure increases during the cis-BR cross-linking. In general, the disappearance of double bonds of cis-1,4-structure and 1,2-structure is in line with our understanding on the crosslinking reaction. However, the reason for the enhancement of double bonds of trans-1,4-structure is unclear for us.

The FTIR spectra in the region 1200–1120 cm^{-1} show the decomposition reaction of DCP with the temperature increasing. In **Figure 2(b)**, the peak at 1152 cm^{-1} is −C−O− stretching of peroxy in DCP, and the intensity of 1152 cm^{-1} obviously decreases from 50 °C to 220 °C. **Figure 3** illustrates the intensity variation at 2852 cm^{-1}, 993 cm^{-1}, 965 cm^{-1}, 910 cm^{-1}, and 738 cm^{-1} from 50 °C to 220 °C. The temperature range of

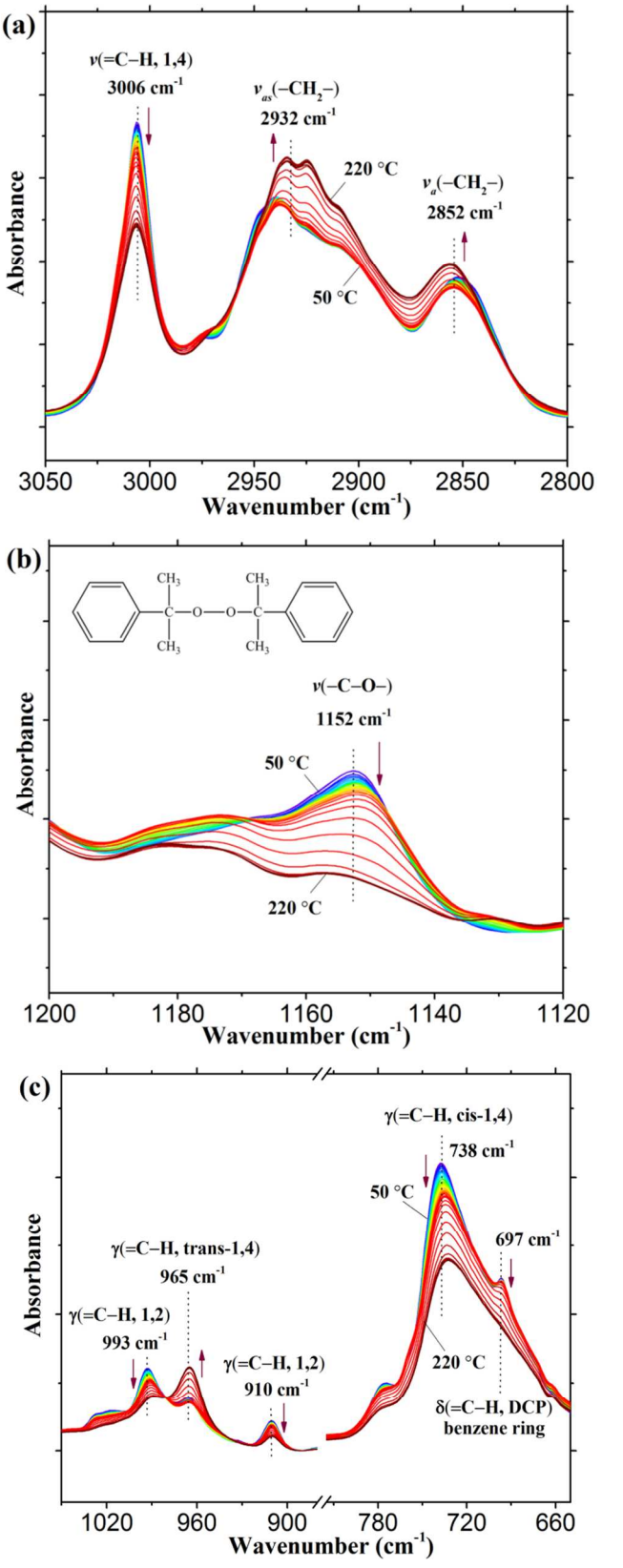

Figure 2. Temperature-dependent FTIR spectra of the cross-linking process of cis-BR from 50 °C to 220 °C. **(a)** 3050–2800 cm^{-1}; **(b)** 1200–1120 cm^{-1}; **(c)** 1000–650 cm^{-1}.

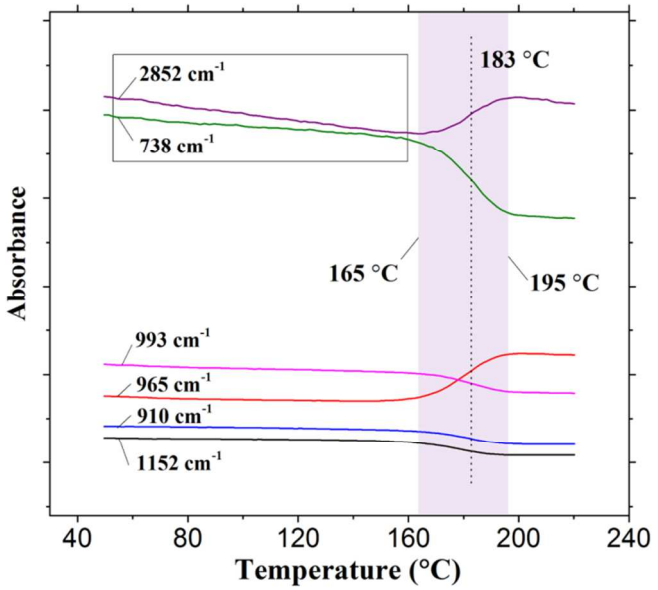

Figure 3. Spectral intensity variation of temperature-dependent FTIR spectra at 2852 cm^{-1}, 1152 cm^{-1}, 993 cm^{-1}, 965 cm^{-1}, 910 cm^{-1}, and 738 cm^{-1} from 50 °C to 220 °C.

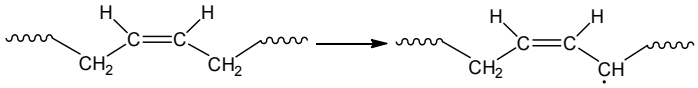

Scheme 2. Generation of –ĊH– macromolecular free radicals via losing α hydrogens of cis-1, 4-structure upon heating.

the cross-linking reaction is determined from 165 °C to 195 °C, which is narrower than that of determined by DSC (146–211 °C). The intensities at 2852 cm^{-1} and 965 cm^{-1} show a great enhancement within 165–195 °C. However, a reduction is observed for 993 cm^{-1}, 910 cm^{-1}, and 738 cm^{-1}. It can be inferred that double bonds of cis-1,4-structure and 1,2-structure are the reactants, and double bonds of trans-1,4-structure and $-CH_2-$ groups are the products during the cross-linking reaction. It also can be observed that the intensity of 993 cm^{-1}, 965 cm^{-1}, 910 cm^{-1} remain unchanged when the temperature is below 165 °C, whereas that of 2852 cm^{-1} and 738 cm^{-1} gradually decreases from 50 °C to 165 °C. The intensity deceasing at 2852 cm^{-1} is the most obvious. As mentioned above, 2852 cm^{-1} is assigned to C–H symmetrical stretching of $-CH_2-$ groups. That is to say, a part of $-CH_2-$ groups are disappeared and transformed into other types of groups. From the viewpoint of thermodynamics, this phenomenon is probably due to the loss of α hydrogens of cis-1, 4-structure (see **Scheme 2**) and the generation of –ĊH– macromolecular free radicals upon heating. This indicates that a large amount of macromolecular free radicals at α position have been generated before the cross-linking reaction. In general, the generation of –ĊH– free radical from 50 °C to 165 °C is still induced by free radicals from the decomposition of DCP. However, DCP decomposition is very weak when the temperature is below 165 °C. So, as shown in **Figure 1** and **Figure 2,** both DSC and in situ FTIR does not detect the DCP decomposition at a low temperature. **Figure 3** also illustrates the intensity variation at 1152 cm^{-1}. We can clearly see that the intensity of 1152 cm^{-1} is constant when the temperature is below 165 °C, which also reveals the much weak of the DCP decomposition. It can interpret the generation of new trans-1, 4-structure during the cross-linking, and free radicals at α position play an important rule (see **Scheme 3**). The generation of trans-1, 4-structure during cis-BR cross-linking with peroxides found here is reported for the first time. Recently, a similar phenomenon has been also found in BR vulcanization with the sulfur by Choi et al,[42] which was called *cis-trans* isomerization of BR. They claimed that the intermediate structure from *cis*-1,4 to *trans*-1,4-structure is the radical formed by the loss of protons at α position. They also calculated the energies of *cis*-1,4, the intermediate structure, and *trans*-1,4-structure using model polymer, and the calculated energies were -490.17, -489.62, and -490.17 kcal/mol, respectively. The intermediate structure is thermodynamically slightly more stable than initial *cis*-1,4-structure, resulting in the *cis-trans* isomerization. Zeng and Ko also reported *cis-trans* isomerization phenomenon. However, in their work, the *cis-trans* transition was observed only at an ultrahigh pressure (>4.0 GPa).[43] In this study, the phenomenon of trans-1,4-structure concentration increasing during the cross-linking (165–195 °C) does not necessarily mean that trans-1,4-structure does not participate in the cross-linking. It is only revealed that the number of trans-1,4-structure converted from cis-1,4 is much higher than that of participating in the cross-linking reaction.

3.3. PCMW2D FTIR spectra

The temperature-dependent FTIR spectra from 50 °C to 220 °C were used to calculated PCMW2D FTIR spectra, and the results are shown in **Figure 4**. PCMW2D contains synchronous and asynchronous spectra, in which the pink areas represent positive correlation intensity, and the blue areas represent the negative. In synchronous PCMW2D FTIR spectra, the positive correlation intensity (pink areas) represents the increasing of the spectral intensity at specific wavenumbers, and the negative correlation intensity (blue areas) shows the decreasing of the spectral intensity at specific wavenumbers. In **Figure 4**, we can clearly see that 2852 cm^{-1} and 965 cm^{-1} present the positive correlation intensity (pink) in synchronous spectra when the temperature is above 158 °C, indicating the increasing of the spectral intensity. This result is identical to the observation in **Figure 3**. In synchronous PCMW2D spectra, the temperature of the cross-linking reaction with maximum rate is determined within 176–183 °C. It is noticed that the temperatures at 2852 cm^{-1}, 993 cm^{-1}, 965 cm^{-1}, 910 cm^{-1}, and 738 cm^{-1} are 183 °C, which is the same as the temperature determined by DSC (183 °C). However, the temperature point at 1152 cm^{-1} is 176 °C, which is the decomposition temperature of DCP. This shows that DSC only can detect the temperature of the cross-linking

reaction, other than the decomposition temperature of DCP. In asynchronous PCMW2D FTIR spectra, the inflection points of the spectral intensity changing can be accurately detected, and the temperature between two inflection points is the temperature range of the reaction at specific wavenumbers. In **Figure 4**, it can be observed that the temperature range of DCP decomposition (1152 cm^{-1}) is from 165 °C to 188 °C, and that of cross-linking reaction is 170 °C to 195 °C.

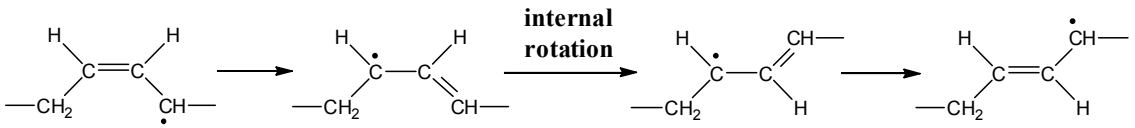

Scheme 3. Generation of new trans-1, 4-structure via the internal rotation during the cross-linking, and free radicals at α position play an important rule.

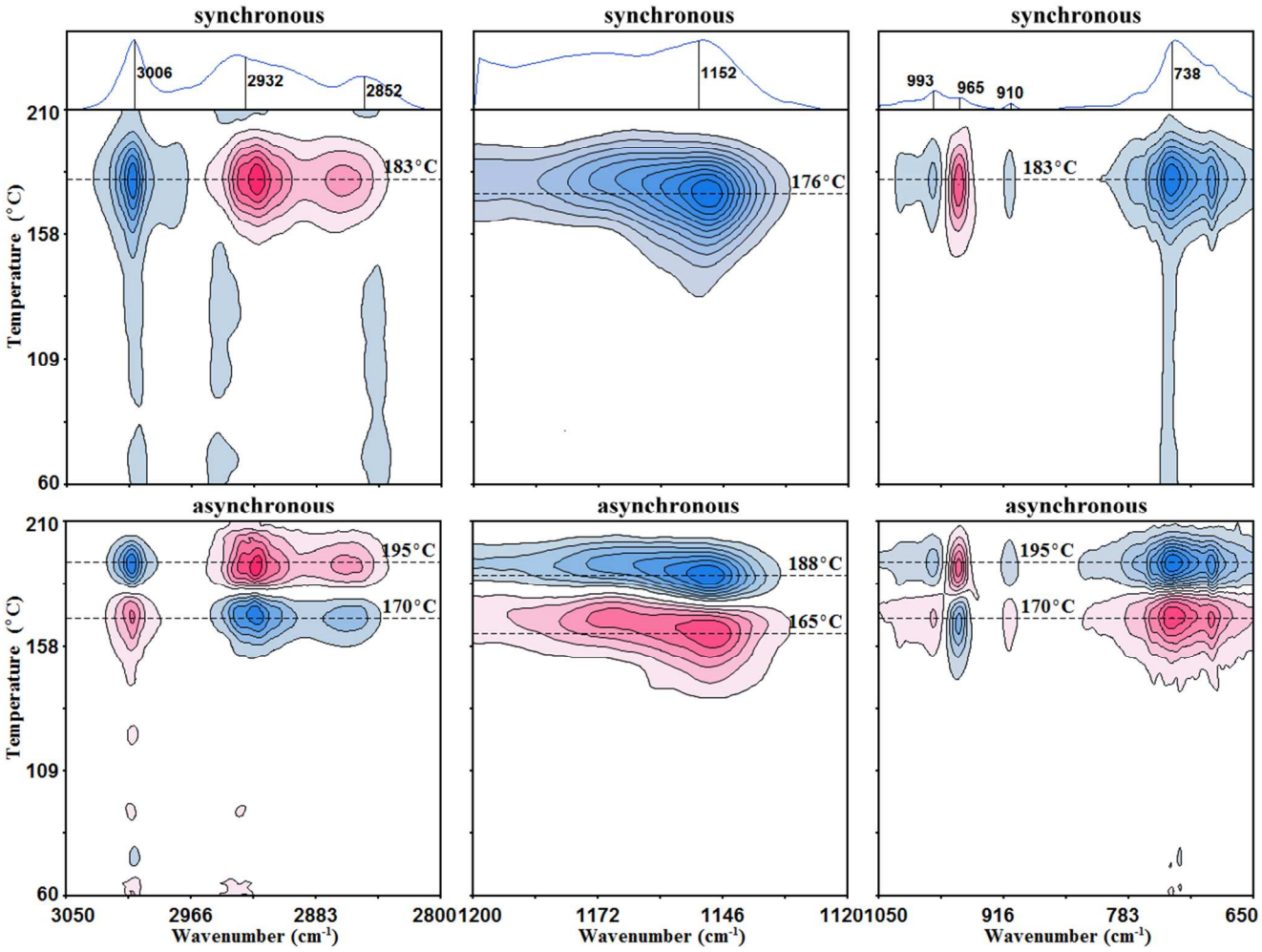

Figure 4. PCMW2D synchronous and asynchronous correlation FTIR spectra in the region 3050–2800 cm^{-1}, 1200–1200 cm^{-1}, and 1050–650 cm^{-1} calculated from the temperature-dependent FTIR spectra from 165 °C to 195 °C. In synchronous spectra, the horizontal dashed lines correspond to the temperature points at 176 °C and 183 °C. In asynchronous spectra, the horizontal dashed lines correspond to the temperature points at 165 °C, 170 °C, 188 °C, 195 °C, respectively. The pink areas represent positive correlation intensity, and the blue areas represent the negative.

3.4. Generalized 2D correlation analysis

To gain a detail mechanism of the cross-linking reaction for cis-BR, the temperature-dependent FTIR spectra within 165-195 °C were used to perform the generalized 2D correlation analysis. The temperature range of 165-195 °C is determined from the asynchronous PCMW2D FTIR spectra in **Figure 4**. The temperature at 165 °C is the lowest point of the temperature range of DCP decomposition, and 195 °C is highest point of the temperature range of the cross-linking reaction. DCP decomposition is an important part of the whole cross-linking reaction. The generalized 2D correlation FTIR spectra are shown in **Figure 5**, **Figure 6**, and **Figure 7**. Generalized 2D FTIR spectra also contain synchronous and asynchronous spectra. The sequential order of the spectral intensity changing at given wavenumber can be conveniently

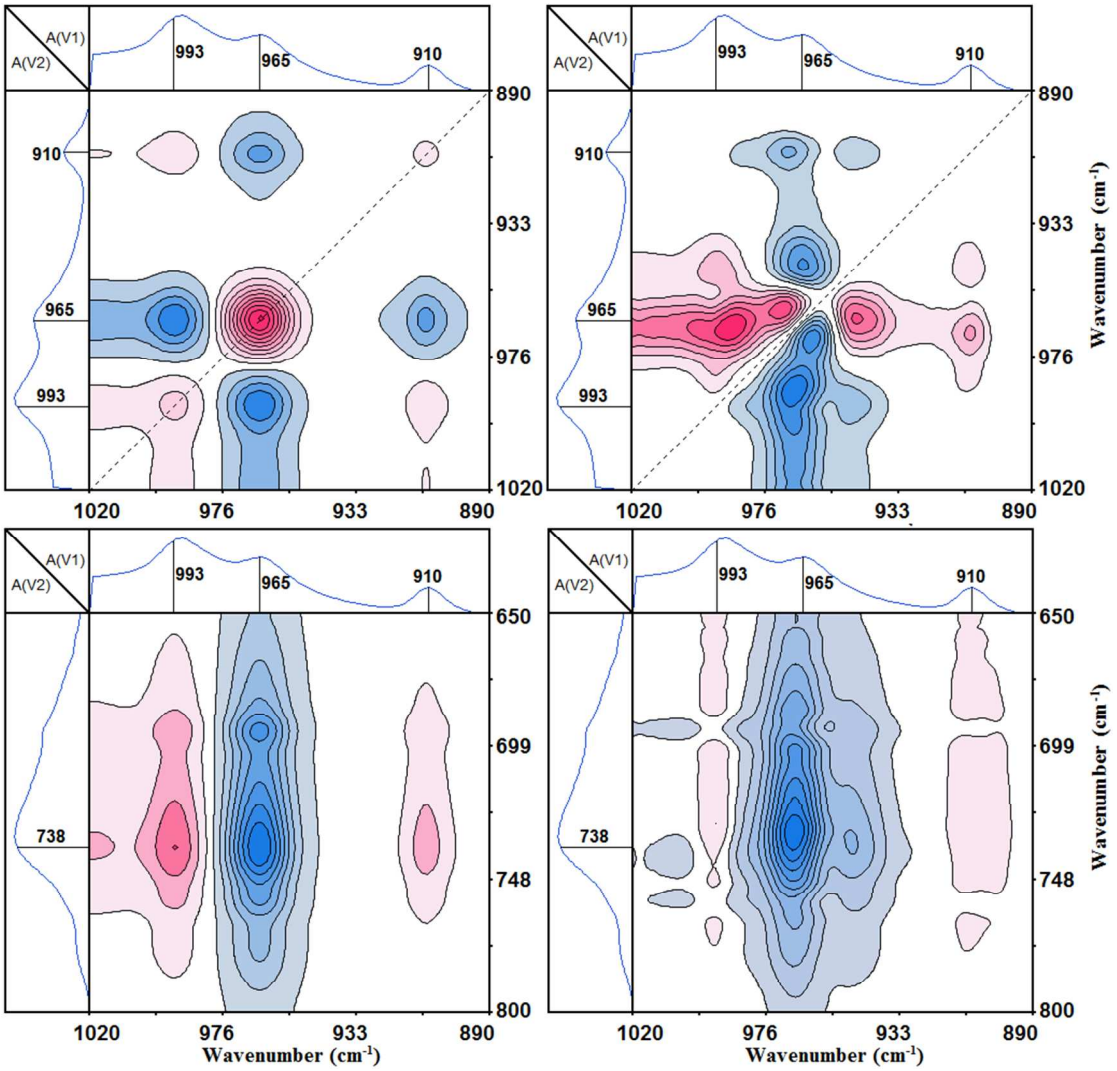

Figure 5. Synchronous (left) and asynchronous (right) FTIR spectra (165−195 °C) in the region 1020−890 cm^{-1} and 1020−890 cm^{-1} *vs* 800−650 cm^{-1}. Pink and blue areas represent the positive and negative correlation intensity, respectively.

judged by the sign of the correlation peaks using Noda's rules. A simple summarization of Noda's rules is as follows:

1) If $\Phi(v_1, v_2)>0$, $\Psi(v_1, v_2)>0$ or $\Phi(v_1, v_2)<0$, $\Psi(v_1, v_2)<0$, then the movement of v_1 is before that of v_2;

2) If $\Phi(v_1, v_2)>0$, $\Psi(v_1, v_2)<0$ or $\Phi(v_1, v_2)<0$, $\Psi(v_1, v_2)>0$, then the movement of v_1 is after that of v_2;

3) If $\Phi(v_1, v_2)>0$, $\Psi(v_1, v_2)=0$ or $\Phi(v_1, v_2)<0$, $\Psi(v_1, v_2)=0$, then the movements of v_1 and v_2 are simultaneous.

3.4.1. Sequential order of different double bonds (cis-1,4-structure, trans-1,4-structure, and 1,2-structure) during the cross-linking

The generalized 2D correlation FTIR spectra in the region 1020-890 cm^{-1} and 1020-890 cm^{-1} *vs* 800-650 $cm^{-1}$are shown in **Figure 5**. The left is the synchronous spectra, and the right is the asynchronous spectra. In **Figure 5,** the pink areas are positive correlation intensity, and the blue areas represent the negative correlation intensity. The sign of the correlation peaks at (993 cm^{-1}, 910 cm^{-1}), (993 cm^{-1}, 965 cm^{-1}), (965 cm^{-1}, 910 cm^{-1}), (993 cm^{-1}, 738 cm^{-1}), (965 cm^{-1}, 738 cm^{-1}), and (910 cm^{-1}, 738 cm^{-1}) are summarized in **Table 2**. According to Noda's rules, the sequential order is 965 cm^{-1}→993 cm^{-1}=910 cm^{-1}→738 cm^{-1}, namely, γ(=C−H, trans-1,4)→γ(=C−H, 1,2)→γ(=C−H, cis-1,4). In the present study, the symbol "→" represents "before", and "←" represents "after". **Figure 5** is generalized 2D correlation FTIR spectra calculated from the temperature-dependent FTIR within 165-195 °C. In **Figure 3**, it can be observed that the intensities of 993 cm^{-1}, 910 cm^{-1}, and 738 cm^{-1} decrease from 165 to 195 °C, whereas that of 965 cm^{-1} obviously increases. The intensity increasing of 965 cm^{-1} indicates the generation of double bonds with trans-1,4-structure. This increasing also reveals double bonds with trans-1,4-structure does not involve in the cross-linking reaction. The double bonds with cis-1,4-structure and 1,2-structure directly take part in the cross-linking, because of the intensity of 993 cm^{-1}, 910 cm^{-1}, and 738 cm^{-1} be decreasing.

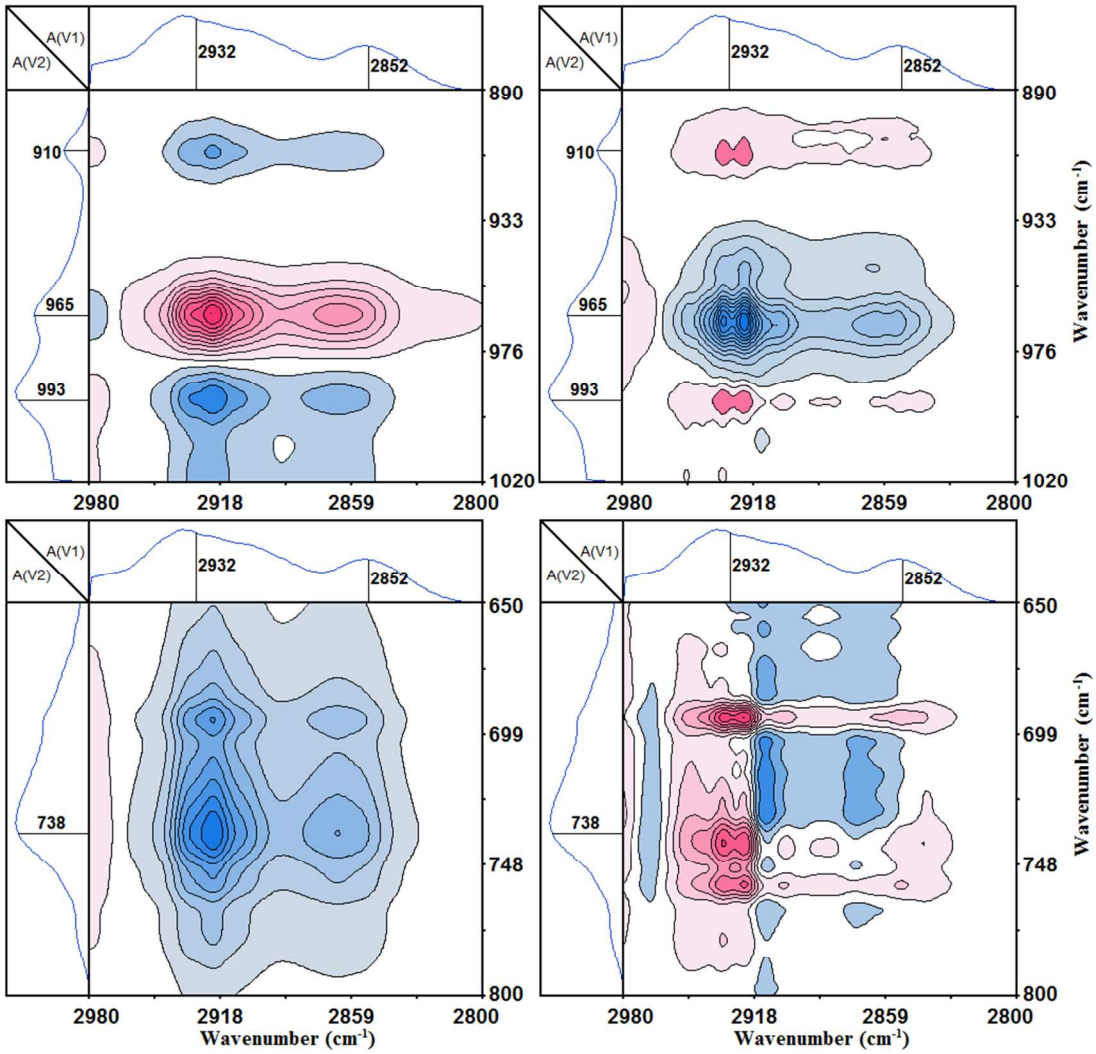

Figure 6. Synchronous (left) and asynchronous (right) FTIR spectra (165−195 °C) in the region 2980−2800 cm^{-1} *vs* 1020−890 cm^{-1} and 2980−2800 cm^{-1} *vs* 800−650 cm^{-1}.

Table 2. Sequential orders of the bands of $-CH_2-$ groups, cis-1,4-structure, trans-1,4-structure, and 1,2-structure, and their cross regions gained from **Figure 5**, **Figure 6**, and **Figure 7**.

Cross correlation peak (cm^{-1}, cm^{-1})	Sign in synchronous spectra	Sign in asynchronous spectra	Sequential order
(993, 910)	+	0	993=910
(993, 965)	-	+	993←965
(965, 910)	-	-	965→910
(993, 738)	+	+	993→738
(965,738)	-	-	965→738
(910, 738)	+	+	910→738
	965 cm^{-1}→993 cm^{-1}=910 cm^{-1}→738 cm^{-1}		
(2852, 910)	-	+	2852←910
(2852, 965)	+	-	2852←965
(2852, 993)	-	+	2852←993
(2852, 738)	-	+	2852←738
(2852, 1152)	-	+	2852←1152
(993, 1152)	+	-	993←1152
(965, 1152)	-	+	965←1152
(910, 1152)	+	-	910←1152
(738, 1152)	+	-	738←1152
	1152 cm^{-1}→965 cm^{-1}→993 cm^{-1}=910 cm^{-1}→738 cm^{-1}→2852 cm^{-1}		
	ν(−C−O−, DCP)→γ(=C−H, trans-1,4)→γ(=C−H, 1,2)→γ(=C−H, cis-1,4)→ν_s($-CH_2-$)		

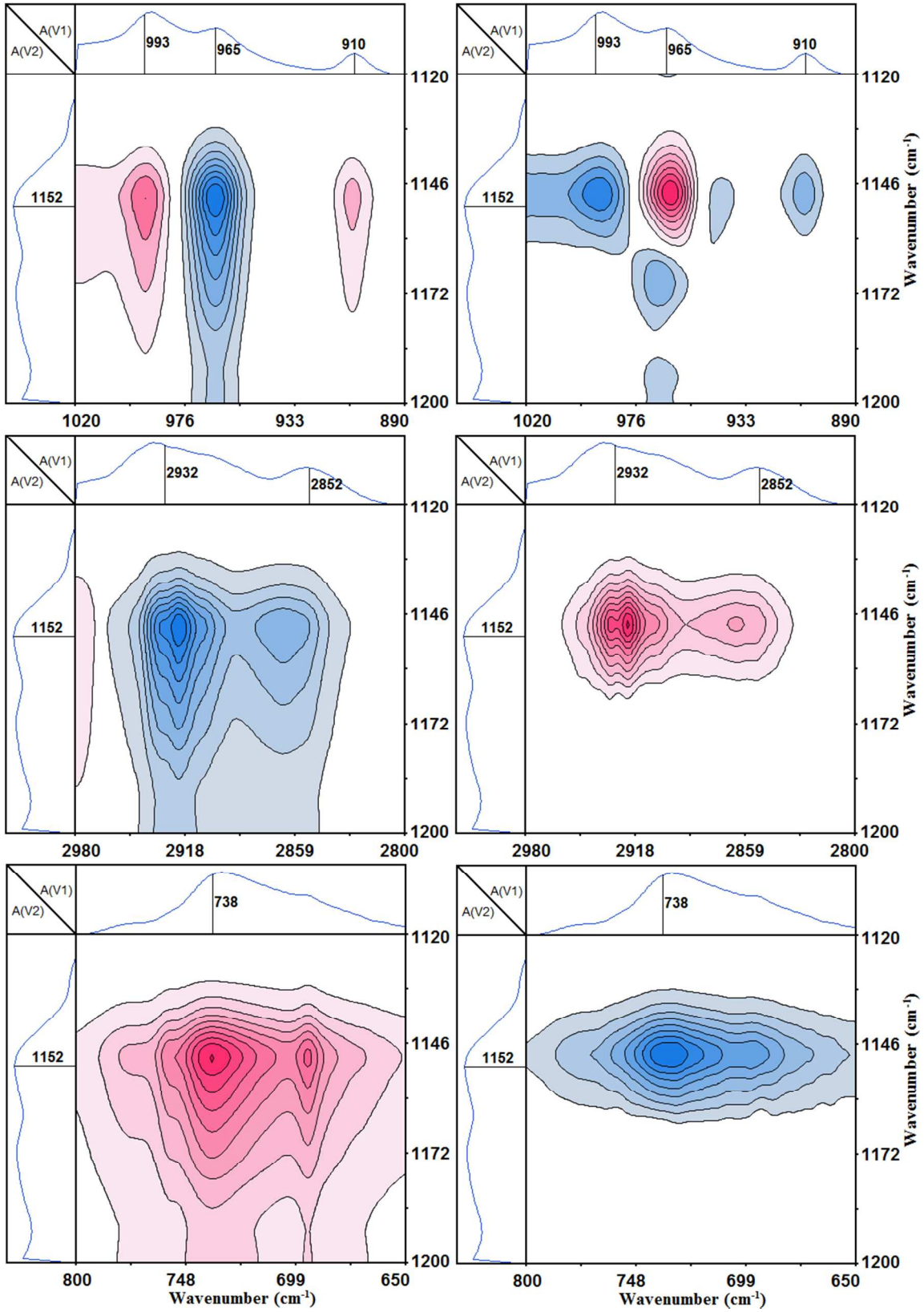

Figure 7. Synchronous (left) and asynchronous (right) FTIR spectra (165–195 °C) in the region 1020–890 cm^{-1} *vs* 1200–1120 cm^{-1}, 2980–2800 cm^{-1} *vs* 1200–1120 cm^{-1}, and 800–650 cm^{-1} *vs* 1200–1120 cm^{-1}.

The sequential orders show that the generation of double bonds with trans-1,4-structure is before the cross-linking of double bonds with 1,2-structure and cis-1,4-structure.

3.4.2. Sequential order of double bonds *vs* $-CH_2-$ groups during the cross-linking

Figure 6 is the generalized 2D correlation FTIR spectra in the region 2980-2800 cm^{-1} *vs* 1020-890 cm^{-1} and 2980-2800 cm^{-1} *vs* 800-650 cm^{-1}. The signs of the corresponding correlation peaks are also summarized in **Table 2**. The sequential orders are 965 $cm^{-1}\rightarrow$2852 cm^{-1}, 993 $cm^{-1}\rightarrow$2852 cm^{-1}, 910 $cm^{-1}\rightarrow$2852 cm^{-1}, and 738 $cm^{-1}\rightarrow$2852 cm^{-1}. In **Figure 3**, an obvious enhancement of the intensity of 2852 cm^{-1} from 165 to 195 °C is observed, which represents the generation of new $-CH_2-$ groups during the cross-linking. According to the sequential orders, it can be inferred the generation of new $-CH_2-$ groups is after the reaction of all the double bonds. These new $-CH_2-$ groups are certainly the products of the cross-linking.

3.4.3. Sequential order of DCP decomposition *vs* double bonds and $-CH_2-$ groups during the cross-linking

Figure 7 is the generalized 2D correlation FTIR spectra in the region 1020−890 cm^{-1} *vs* 1200−1120 cm^{-1}, 2980−2800 cm^{-1} *vs* 1200−1120 cm^{-1}, and 800−650 cm^{-1} *vs* 1200−1120 cm^{-1}. **Table 2** lists the sign of the corresponding correlation peaks. According to Noda's rules, the sequential orders are 2852 $cm^{-1}\leftarrow$1152 cm^{-1}, 993 $cm^{-1}\leftarrow$1152 cm^{-1}, 965 $cm^{-1}\leftarrow$1152 cm^{-1}, 910 $cm^{-1}\leftarrow$1152 cm^{-1}, and 738 $cm^{-1}\leftarrow$1152 cm^{-1}. This indicates that the DCP decomposition is before all the reactions of the double bonds and the generation of $-CH_2-$

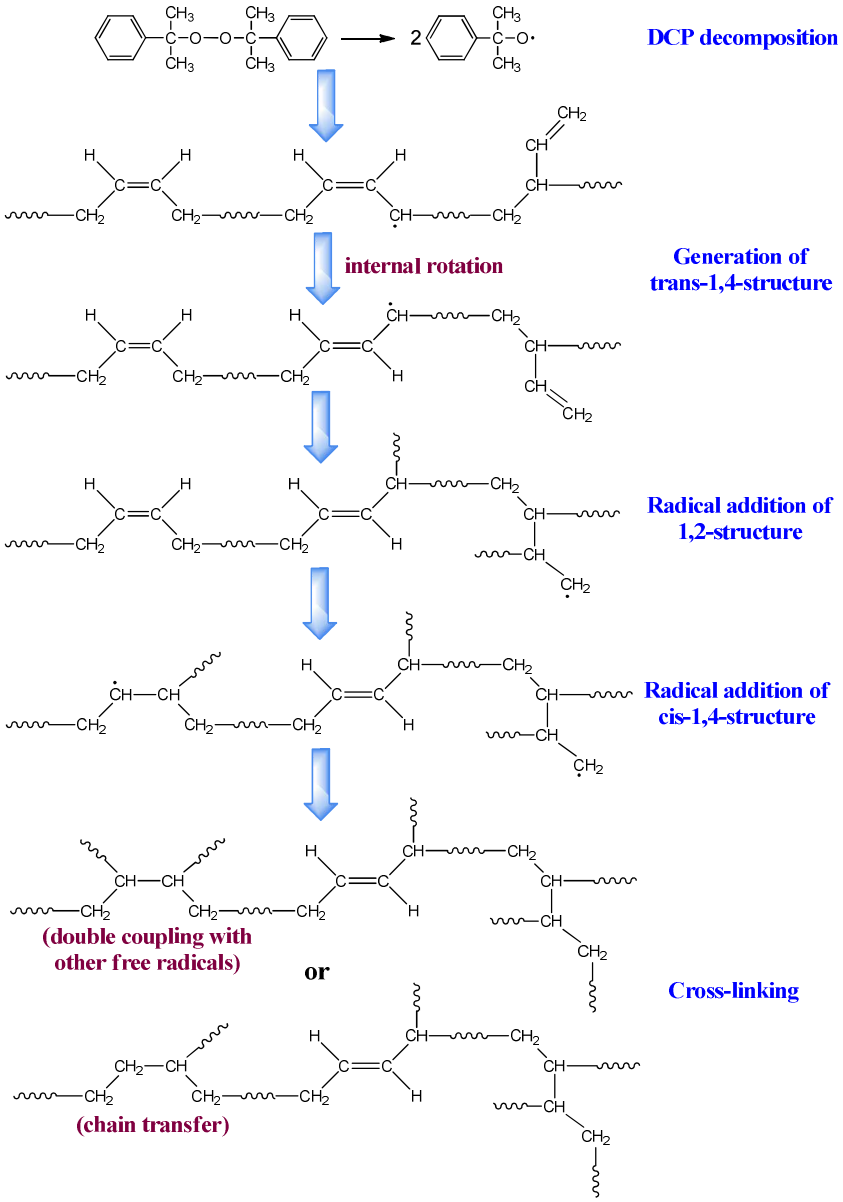

Scheme 4. Five-steps process of cis-BR cross-linking with DCP inferred from the 2D correlation analysis.

groups. Thus, it is learned that DCP decomposition is the first step during the whole cross-linking.

The whole sequential orders of cis-BR cross-linking from 165 to 195 °C is summarized as 1152 cm^{-1}→965 cm^{-1}→993 cm^{-1}=910 cm^{-1}→738 cm^{-1}→2852 cm^{-1}. The corresponding group movements are ν(−C−O−, DCP)→γ(=C−H, trans-1,4)→γ(=C−H, 1,2)→γ(=C−H, cis-1,4)→ν_s(−CH_2−). There have 5 steps can be summed up during the whole cross-linking process. The first step is the DCP decomposition and the free radicals releasing. The second step is the generation of trans-1,4-structure, and we think this phenomenon probably due to the internal rotation of cis-1,4-structure induced by free radicals at α position. This step actually does not participate in the final cross-linking, and we prefer to assign it as a side reaction. The third step is the free radical addition of double bonds with 1,2-structure, and then the fourth step is the free radical addition of double bonds with cis-1,4-structure. It also reveals that the radical addition of 1,2-structure is more easily than that of cis-1,4-structure. The final step is the cross-linking via double coupling of two macromolecular free radicals. The free radicals from cis-1,4-structure also can be probably terminated by a chain transfer, resulting in the generation of a part of new −CH_2− groups. This 5-steps process of cross-linking is illustrated in **Scheme 4.**

4. Conclusions

In the present study, the cross-linking process of cis-BR induced by peroxide was studied by in situ FTIR spectra combined with PCMD2D and generalized 2D correlation spectroscopy. DSC was also employed to detect the temperature region of the cross-linking process. The cross-linking temperature with a maximum rate was determined at 183 °C via PCMW2D correlation FTIR spectra, which is identical with the DSC results. The temperature region of the cis-BR cross-linking determined by PCMW2D was within 165-195 °C. The generation of –ĊH− macromolecular free radicals through losing α hydrogens was observed when the temperature was below 165 °C. It was found an abnormal increasing of double bonds with trans-1,4-structure during the cross-linking process (165-195 °C). The generation of new trans-1,4-structure was probably due to the internal rotation, and free radicals at α position play an important rule. We also found an obvious enhancement of −CH_2− groups during the cis-BR cross-linking (165-195 °C), which indicated that a large part of the double bonds with cis-1, 4- and 1, 2-structrue involved in cross-linking is transformed to −CH_2− groups.

To gain a detail mechanism of cis-BR cross-linking within 165-195 °C, generalized 2D correlation analysis was performed. The sequential orders of group movements showed a 5-steps process for the whole cross-linking:

1) DCP decomposition and the free radicals releasing;
2) Generation of trans-1,4-structure due to the internal rotation of cis-1,4-structure induced by free radicals at α position;
3) Free radical addition of double bonds with 1,2-structure;
4) Free radical addition of double bonds with cis-1,4-structure;
5) Cross-linking via double coupling of two macromolecular free radicals. The free radicals from cis-1,4-structure also can be probably terminated by a chain transfer.

Acknowledgements

This work was supported by the National Natural Science Foundation of China (Grant Nos. 51473104, 51003066), State Key Laboratory of Polymer Materials Engineering (Grant No. sklpme2014-3-06), and the Outstanding Young Scholars Foundation of Sichuan University (Grant No. 2011SCU04A13).

Notes and references

[a] State Key Laboratory of Polymer Materials Engineering of China, Polymer Research Institute, Sichuan University, Chengdu 610065, China

[b] the Technology Research Center of Polymer Materials Engineering of Tai'an, Longteng Polymer Materials Co., Ltd., Tai'an 271000, China

*Corresponding author. Tel.: +86-28-85402601; Fax: +86-28-85402465; E-mail address: zhoutaopoly@scu.edu.cn (T. Zhou) or amzhang215@vip.sina.com (A. Zhang)

1. M. Morton, J. Macromol. Sci. A, 1981, **15**, 1289-1302.
2. E. Schoenberg, H. A. Marsh, S. J. Walters and W. M. Saltman, Rubber Chem. Technol., 1979, **52**, 526-604.
3. M. Akiba and A. S. Hashim, Prog. Polym. Sci., 1997, **22**, 475-521.
4. M. Rubinstein and S. Panyukov, Macromolecules, 2002, **35**, 6670-6686.
5. W. Salgueiro, A. Marzocca, A. Somoza, G. Consolati, S. Cerveny, F. Quasso and S. Goyanes, Polymer, 2004, **45**, 6037-6044.
6. A. M. Zaper and J. L. Koenig, Rubber Chem. Technol., 1987, **60**, 252-277.
7. L. D. Loan, Journal of Polymer Science Part A: General Papers, 1964, **2**, 3053-3066.
8. R. A. Dickie and J. D. Ferry, J. Phys. Chem., 1966, **70**, 2594-2600.
9. L. González, A. Rodríguez, A. Marcos and C. Chamorro, Rubber Chem. Technol., 1996, **69**, 203-214.
10. R. Rajan, S. Varghese and K. E. George, Rubber Chem. Technol., 2013, **86**, 488-502.
11. A. Thitithammawong, C. Nakason, K. Sahakaro and J. Noordermeer, Polym. Test., 2007, **26**, 537-546.
12. L. D. Loan, Rubber Chem. Technol., 1967, **40**, 149-176.
13. R. G. Mancke and J. D. Ferry, Transactions of The Society of Rheology (1957-1977), 1968, **12**, 335-350.
14. T. R. Manley and M. M. Qayyum, Polymer, 1971, **12**, 176-188.
15. R. S. Clough and J. L. Koenig, Journal of Polymer Science Part C: Polymer Letters, 1989, **27**, 451-454.
16. G. Padmavathi, M. G. Mandan, S. P. Mitra and K. K. Chaudhuri, Comput. Chem. Eng., 2005, **29**, 1677-1685.

17. I. Noda, Appl. Spectrosc., 1993, **47**, 1329-1336.
18. M. Thomas and H. H. Richardson, Vib. Spectrosc., 2000, **24**, 137-146.
19. S. Morita, H. Shinzawa, I. Noda and Y. Ozaki, Appl. Spectrosc., 2006, **60**, 398-406.
20. S. Morita, K. Kitagawa, I. Noda and Y. Ozaki, J. Mol. Struct., 2008, **883–884**, 181-186.
21. Z. W. Wang and P. Y. Wu, RSC Adv., 2012, **2**, 7099-7108.
22. S. Sun, H. Tang, P. Wu and X. Wan, Phys. Chem. Chem. Phys., 2009, **11**, 9861-9870.
23. L. Hou and P. Y. Wu, RSC Adv., 2014, **4**, 39231-39241.
24. T. Zhou, Z. Wu, Y. Li, J. Luo, Z. Chen, J. Xia, H. Liang and A. Zhang, Polymer, 2010, **51**, 4249-4258.
25. T. Zhou, A. Zhang, C. Zhao, H. Liang, Z. Wu and J. Xia, Macromolecules, 2007, **40**, 9009-9017.
26. H. Lai and P. Wu, Polymer, 2010, **51**, 1404-1412.
27. J. Luo, T. Zhou, X. Fu, H. Liang and A. Zhang, Eur. Polym. J., 2011, **47**, 230-237.
28. M. Wang and P. Wu, Polymer, 2011, **52**, 769-777.
29. Y. Liu, W. Li, L. Hou and P. Wu, RSC Adv., 2014, **4**, 24263-24271.
30. H. Lee, Y. M. Jung, K. I. Lee, H. S. Kim and H. S. Park, RSC Adv., 2013, **3**, 25944-25949.
31. Y. Shen and P. Wu, J. Mol. Struct., 2008, **886**, 72-76.
32. Z. G. Chen, T. Zhou, J. T. Hui, L. Li, Y. Y. Li, A. M. Zhang and T. Y. Yuan, Vib. Spectrosc., 2012, **62**, 299-309.
33. Y. Y. Li, T. Zhou, Z. G. Chen, J. T. Hui, L. Li and A. M. Zhang, Polymer, 2011, **52**, 2059-2069.
34. Y. C. Liu, T. Zhou, Z. G. Chen, L. Li, Y. H. Zhan, A. M. Zhang and F. W. Liu, Polym. Advan. Technol., 2014, **25**, 760-768.
35. T. Zhou, Y. C. Liu, L. L. Peng, Y. H. Zhan, F. W. Liu, A. M. Zhang and L. Li, Anal. Bioanal. Chem., 2014, **406**, 4157-4172.
36. T. Zhou, L. L. Peng, Y. C. Liu, Y. H. Zhan, F. W. Liu and A. M. Zhang, Vib. Spectrosc., 2014, **70**, 137-161.
37. I. Noda and Y. Ozaki, Two-Dimensional Correlation Spectroscopy – Applications in Vibrational and Optical Spectroscopy, John Wiley & Sons, Ltd, Chichester, 2004.
38. J. Guilment and L. Bokobza, Vib. Spectrosc., 2001, **26**, 133-149.
39. E. Serrano, A. Zubeldia, M. Larranaga, P. Remiro and I. Mondragon, Polym. Degrad. Stabil., 2004, **83**, 495-507.
40. N. C. Craig, K. A. Hanson, R. W. Pierce, S. D. Saylor and R. L. Sams, J. Mol. Spectrosc., 2004, **228**, 401-413.
41. I. Di Somma, R. Marotta, R. Andreozzi and V. Caprio, J. Hazard. Mater., 2011, **187**, 157-163.
42. S.-S. Choi, Y. Kim and H.-M. Kwon, RSC Adv., 2014, **4**, 31113-31119.
43. X.-R. Zeng and T.-M. Ko, J. Appl. Polym. Sci., 1998, **67**, 2131-2140.

